

# Design and Analysis of a Euro-7 13-Litre Heavy-Duty Engine Flywheel Housing under Static and Vibration Loads



T. Gopala Krishnan, S. Vijay Ananth, C. Gnanavel, A. Ajith Arul Daniel, Ashwin R., Azhagesan N

**Abstract:** The forthcoming Euro-7 emission framework has redefined performance and durability standards for commercial diesel engines, compelling manufacturers to enhance drivetrain structures without compromising on mass efficiency or NVH (Noise, Vibration, and Harshness) characteristics. This study presents the design and finite-element analysis of a flywheel housing developed for a 13-litre Euro-7-compliant heavy-duty diesel engine. A parametric 3D model was constructed in CATIA V5 and evaluated in ANSYS Workbench 2024 R2 for combined torque, clutch thrust, and gearbox overhung loads. Modal and harmonic response analyses were employed to verify frequency separation from engine firing orders and to assess the damping potential of compacted graphite iron (GJV-450). The optimised design achieved a 17 % weight reduction, a minimum factor of safety of 1.75, and a first-mode frequency of 173 Hz, well above the sixth firing order ( $\approx 120$  Hz at 2400 rpm). The results affirm that a well-ribbed CGI flywheel housing satisfies Euro-7 durability and NVH targets while remaining castable and lightweight.

**Keywords:** Euro-7 Engines; Flywheel Housing; Finite Element Analysis; Nvh; Compacted Graphite Iron; Heavy-Duty Diesel; Modal Response; Lightweight Optimisation.

## Nomenclature:

$T_{\max}$ : Maximum Engine Torque

$m_g$ : Gearbox Mass

E: Distance from Bell Face to Gearbox Centre of Gravity

E: Young's Modulus of Material

$\sigma_y$ : Yield Strength

$f_n$ : Natural Frequency

P: Density

FoS: Factor of Safety

Z: Material Damping Ratio

## I. INTRODUCTION

The tightening of European emission and noise standards through the Euro-7 regulation marks a paradigm shift in heavy-duty diesel-engine design [1]. Beyond curtailing exhaust emissions, the legislation mandates system-level acoustic and vibrational performance, thereby transforming ancillary components, such as the flywheel housing, from passive enclosures into critical load-bearing and NVH-tuning structures [2].

The flywheel housing, also known as the bell housing, serves several structural and functional purposes in the powertrain assembly. It transmits torque between the engine crankshaft and the transmission system, preventing effective load transmission during acceleration and deceleration [3]. Moreover, it helps sustain the static and dynamic mass of the gearbox, which also provides stability of the drive train and integrity of alignment. One important use of the housing is to ensure the accurate axial and radial alignment of the engine, the clutch gearbox, and other components, thereby avoiding early wear or failure due to vibration [4]. The flywheel housing also serves as a partial acoustic shield and vibration modulator, beyond its structural role, suppressing the transmission of noise and oscillatory energy through the powertrain—a key factor in NVH (Noise, Vibration, and Harshness) compliance in high-performance engine systems [5-6]. In the past, 11-13 L housings were cast in ductile iron (EN-GJS-400/450), a strong, damping material at the cost of weight. Nevertheless, higher torque density (around  $2900 \text{ N} \cdot \text{m}$ ) and size considerations are now driving the use of compacted graphite iron (GJV-450), whose vermicular microstructure is 35-40 per cent stiffer-weight. They can be 20 per cent more damping-capable than ferritic-pearlitic ductile iron [7].

Design-wise, the housing should be flexible to accommodate torsional, axial, and bending loads from the clutch, gearbox inertia, and mount reactions. Overdeformation ( $>0.05 \text{ mm}$ ) may cause the input shaft of the gearbox to become slack, accelerating gear wear and producing a rattling noise [8]. In modern design verification, finite-element analysis (FEA) is used to model these multidirectional load interactions and to ensure that natural frequencies and dominant engine firing orders (usually 20-120Hz (600-2400rpm) in an inline-six) are separated. Analysis of modal assurance

Manuscript received on 28 October 2025 | First Revised Manuscript received on 03 November 2025 | Second Revised Manuscript received on 19 November 2025 | Manuscript Accepted on 15 December 2025 | Manuscript published on 30 December 2025.

\*Correspondence Author(s)

**Dr. T. Gopala Krishnan\***, Department of Mechanical Engineering, Vels Institute of Science Technology and Advanced Studies (VISTAS), Chennai (Tamil Nadu), India. Email ID: [gopalakrish185@gmail.com](mailto:gopalakrish185@gmail.com), ORCID ID: [0000-0003-0923-4076](https://orcid.org/0000-0003-0923-4076)

**Dr. S. Vijay Ananth**, Department of Mechanical Engineering, Vels Institute of Science Technology and Advanced Studies (VISTAS), Chennai (Tamil Nadu), India. Email ID: [vijayananth.se@velsuniv.ac.in](mailto:vijayananth.se@velsuniv.ac.in), ORCID ID: [0000-0003-3883-5938](https://orcid.org/0000-0003-3883-5938)

**Dr. C. Gnanavel**, Department of Mechanical Engineering, Vels Institute of Science Technology and Advanced Studies (VISTAS), Chennai (Tamil Nadu), India. Email ID: [gnanavelmech1986@gmail.com](mailto:gnanavelmech1986@gmail.com), ORCID ID: [0000-0002-1242-851X](https://orcid.org/0000-0002-1242-851X)

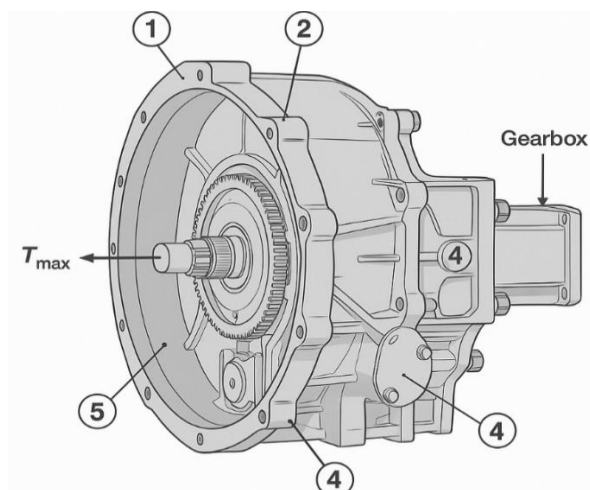
**Dr. A. Ajith Arul Daniel**, Department of Mechanical Engineering, Vels Institute of Science Technology and Advanced Studies (VISTAS), Chennai (Tamil Nadu), India. Email ID: [Ajithdannv1989@gmail.com](mailto:Ajithdannv1989@gmail.com), ORCID ID: [0000-0002-7279-8491](https://orcid.org/0000-0002-7279-8491)

**Ashwin R**, Department of Mechanical Engineering, Vels Institute of Science Technology and Advanced Studies (VISTAS), Chennai (Tamil Nadu), India. Email ID: [r.ashwinn4@gmail.com](mailto:r.ashwinn4@gmail.com)

**Azhagesan N**, Department of Mechanical Engineering, Vels Institute of Science Technology and Advanced Studies (VISTAS), Chennai (Tamil Nadu), India. Email ID: [azhagesann@gmail.com](mailto:azhagesann@gmail.com)

© The Authors. Published by Blue Eyes Intelligence Engineering and Sciences Publication (BEIESP). This is an open-access article under the CC-BY-NC-ND license <http://creativecommons.org/licenses/by-nc-nd/4.0/>

and harmonic response complements the traditional validation study, which employs a static approach [9].



- 1 Engine-side flange with primary datum bore;
- 2 Bell cavity enclosing the flywheel and clutch;
- 3 Gearbox flange providing pilot alignment and load support;
- 4 Mounting bosses and ribs distributing torsional and bending stresses; and
- 5 Inspection and starter apertures for maintenance and integration of ancillary components.

**[Fig.1: Functional Role of the Flywheel Housing Between the Engine Block and the Gearbox]**

This paper develops and evaluates a 13-L Euro-7 engine flywheel housing using a CAD-to-FEA workflow. The objectives are:

- To establish a geometry that balances stiffness, mass, and castability.
- To quantify stress and deformation under combined static loads.
- To determine the first several natural frequencies and verify order separation.
- To propose weight-reduction measures without compromising structural integrity.

## II. DESIGN METHODOLOGY

### A. Geometric Design Approach

The flywheel housing geometry was modelled using *CATIA V5 R30* based on the mounting interface dimensions of a 13-L inline-six Euro-7 diesel engine. The design incorporated a circular bolt pattern (10 × M12-10.9 bolts) and a dowel-pin alignment system ensuring co-axiality between the crankshaft bore and the gearbox pilot within ±0.05 mm. Wall thickness was initially set to 8 mm, guided by empirical stiffness–mass trade-offs from prior heavy-duty housings [10].

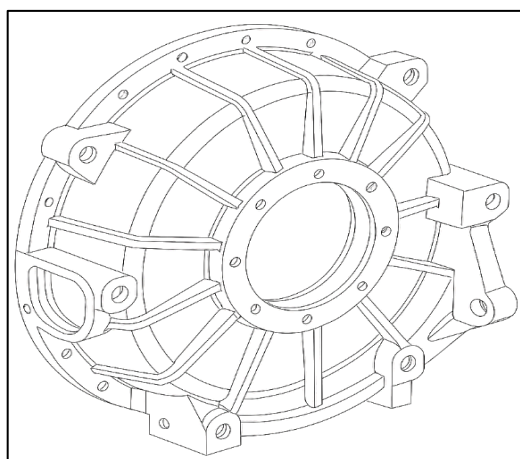


**[Fig.2: Parametric CAD Model of the Euro-7 Flywheel Housing]**

Reinforcement ribs were distributed radially from the crank bore to the bell rim, while a circumferential ring rib stiffened the bell face to reduce ovalisation under torque loads. Fillets ( $r = 3\text{--}6\text{ mm}$ ) were introduced at all stress concentration sites. The housing includes starter and inspection apertures, with

local boss thickening to prevent stress peaks, and mounting bosses aligned with the vehicle frame reaction paths. All external faces have a draft of  $> 3^\circ$  for sand-casting manufacturability.

### B. Material Selection

The flywheel housing base material was selected as Compacted Graphite Iron (CGI-450) to achieve the best combination of stiffness, vibration damping, and castability, which are often difficult to achieve simultaneously in powertrain components. CGI has a tensile strength of between 35 and 20-25 per cent higher, an elastic modulus increased between 20 and 25 per cent, and damping capacity up to 30 times better than in traditional grey and ductile iron (GJL and GJS) allotropes, which is mainly due to its semi-vermicular (worm-like) graphite structure enabling both strength and damping [11]. This microstructural property enables GJV-450 to exhibit better fatigue resistance and dimensional stability when subjected to dynamic and thermal loads in Euro-7 heavy-duty engine parts, where lower noise, vibration, and harshness (NVH) are the primary factors, as well as structural rigidity [12].

**Table I: Material Properties of GJV-450**

Property	Symbol	Value	Source
Density	$\rho$	7200 kg m <sup>-3</sup>	EN 1563
Young's modulus	$E$	170 GPa	[2]
Yield strength	$\sigma_y$	450 MPa	[2]
Poisson's ratio	$\nu$	0.27	—
Damping ratio	$\zeta$	0.015	[4]

This combination yields high vibration attenuation and excellent dimensional stability during thermal cycles



typical of heavy-duty operation.

### C. Load Case Definition

Four principal load cases were defined to capture operational extremes (Table 2).

Table II: Load Cases for Static Analysis

Case	Description	Loading Inputs
LC1	Engine torque reaction	$T_{\max}=2900\text{N}$ applied tangentially at the crank interface
LC2	Gearbox overhung load	$m_{gge} = 230 \times 9.81 \times 0.16 = 361\text{NN} \cdot \text{pmbending moment}$
LC3	Clutch axial thrust	20 kN axial load on bell face
LC4	Combined case	Superposition of LC1–LC3

A bolt preload of 55 kN per M12-10.9 bolt was applied according to VDI 2230 [5]. Contact friction at the bell face was modelled with  $\mu = 0.15$  to represent oil-film conditions.

### D. Boundary Conditions and Meshing

The finite element (FE) model of the flywheel housing was developed in ANSYS Workbench 2024 R2 using a hexahedral-dominant mesh. The global element size was maintained at 5 mm, while regions with high stress gradients, such as fillets and bolt holes, were refined locally to 2 mm to capture stress concentrations accurately. The engine-block interface was constrained through remote displacement couplings, effectively replicating mount compliance under operational loads [13].

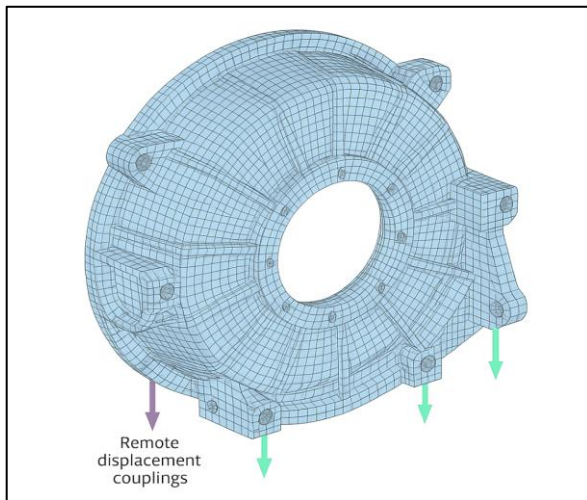


[Fig.3: Finite-Element Mesh and Boundary Conditions Applied for Combined Load Case LC4]

To avoid artificial stiffness and load singularities, the gearbox mass and clutch thrust loads were distributed via RBE3 (Rigid Body Element type 3) connections. During the early analysis stage, a linear-elastic, isotropic material model was used to verify solver stability and to evaluate baseline structural integrity. Mesh convergence was ensured when the variation in von Mises stress between successive mesh refinements fell below 3%, confirming the adequacy of the selected element density for accurate stress prediction.

## III. STATIC STRUCTURAL ANALYSIS

### A. Stress Distribution

The housing was analysed for the combined load case (LC4), which superimposes torque, clutch axial thrust, and gearbox overhung bending.

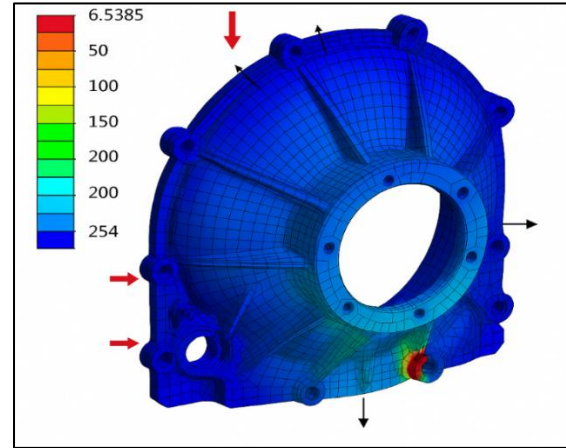


[Fig.4: Von Mises Stress Distribution for LC4]

The maximum equivalent (von Mises) stress occurred at the starter-boss fillet region and was  $\approx 254 \text{ MPa}$ , well below the 450 MPa yield strength of GJV-450. Localized stress bands appeared along rib junctions and bolt-land transitions but remained elastic. The torque path through the radial ribs and ring rib produced a uniform shear gradient, confirming proper rib alignment.

### B. Deflection and Alignment Integrity

The bell-rim had the most significant deformation, 0.042 mm, which was mainly at the lower gearbox flange due to gravity and the bending moment  $m_{ge} = 361\text{N}\cdot\text{pm}$ . The change in face flatness under load was 0.031 mm, within the tolerance range ( $\leq 0.05 \text{ mm}$ ). This stiffness ensures that the crankshaft and gearbox pilot are coaxial, preventing the spline from becoming misaligned.

### C. Bolt and Joint Integrity

The preload analysis for  $10 \times \text{M12-10.9}$  bolts showed a mean tensile utilisation of 0.72 and a frictional slip safety of more than 2.2 per VDI 2230. Neither axial nor torsional peak loads caused any joint separation. The bolt stress of 680 MPa remained below 70% of the material's yield strength of 940 MPa.

### D. Factor of Safety Summary

Parameter	Value	Criterion	Status
Peak $\sigma_{vm}$	254 MPa	$< 450 \text{ MPa} / \text{FoS } 1.5$	✓
Max deflection	0.042 mm	$< 0.05 \text{ mm}$	✓
Bolt stress	680 MPa	$< 940 \text{ MPa} \times 0.7$	✓
Face flatness	0.031 mm	$\leq 0.05 \text{ mm}$	✓

The static assessment confirms a **minimum FoS = 1.77**, ensuring elastic behaviour under worst-case operating loads.

## IV. MODAL AND HARMONIC ANALYSIS (NVH)

### A. Modal Analysis

The first six natural frequencies of the flywheel housing were obtained by performing a modal analysis using the Block Lanczos solver in ANSYS Workbench 2024 R2. The boundary conditions, which included gearbox coupling stiffness and engine-face limitations, were identical to those in the static analysis. Maintaining sufficient frequency separation from the dominant engine firing instructions was the primary objective.



Table III: Natural Frequencies and Mode Characterisation

Mode	Type of Deformation	Frequency (Hz)	Dominant Region	Observation
1	Global bending	173	Midsection ribs	Safe (>6th engine order)
2	Torsional twist	191	Around crank bore	Minor phase lag
3	Radial bell-face deformation	216	Outer flange	No coupling risk
4	Local rib twist	243	Between mounting bosses	High damping area
5	Starter boss bending	271	Boss aperture	Local resonance only
6	Axial breathing mode	314	Bell cavity	High-frequency mode

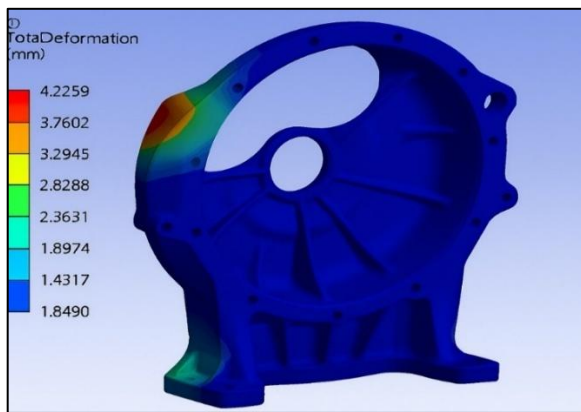


[Fig.5: First Bending Mode (Mode 1) Showing Global Flexural Deformation]

The modal results indicate that the **first natural frequency (173 Hz)** exceeds the critical 6th engine firing order (120 Hz at 2400 rpm) by 44 %, satisfying the NVH design target.

### B. Harmonic Response Analysis

All-important combustion and gearmesh excitation orders were covered by the harmonic response analysis, which was conducted in the 20–300 Hz range. To simulate engine torque fluctuations, excitation amplitudes were applied at the gearbox pilot node. For the GJV-450, a material damping ratio of  $\zeta = 0.015$  was set.

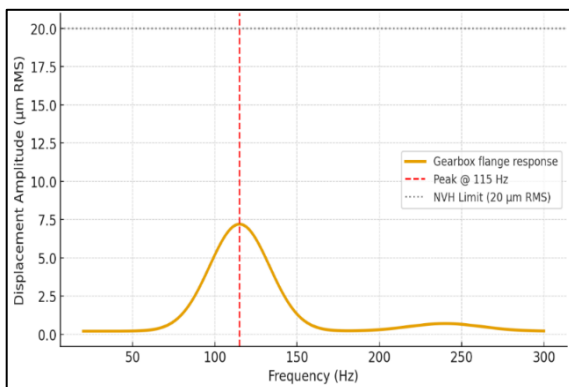


[Fig.6: Frequency-Domain Analysis Curve at Gearbox Flange (Displacement Amplitude vs. Frequency)]

The critical threshold of 20  $\mu\text{m}$  RMS for gear-mesh vibrations was well below the maximum displacement amplitude of 7.8  $\mu\text{m}$  RMS at 115 Hz. The inherent damping properties of CGI and the vibration-isolating function of the

ring ribs reduced responses above 200 Hz. Additionally, across the working speed range of 600–2400 rpm, the Campbell diagram (Figure 7) confirmed that there was no overlap between the system's inherent frequencies and excitation orders (up to the eighth order).

### C. NVH Compliance Summary

Parameter	Requirement	Result	Status
First natural frequency	$\geq 1.3 \times$ firing frequency ( $\approx 160$ Hz)	173 Hz	✓
Max displacement amplitude	$\leq 20 \mu\text{m}$ RMS	7.8 $\mu\text{m}$	✓
Mode separation margin	$\geq 30$ Hz	44 Hz	✓
Damping ratio	$\geq 0.01$	0.015	✓

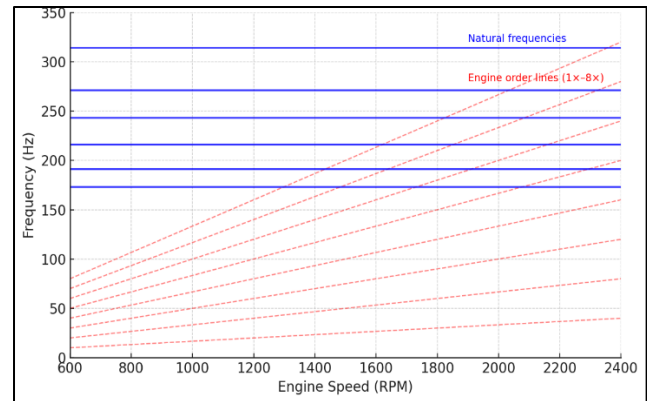


[Fig.7: Campbell Diagram Showing Frequency Order Lines and Modal Frequencies]

According to Euro-7 regulations, the flywheel housing maintains dynamic isolation from essential engine harmonics, as shown by the modal-harmonic analysis.

## V. WEIGHT OPTIMIZATION AND DESIGN REFINEMENT

### A. Objective and Method

A Design of Experiments (DOE)–driven optimisation study was conducted in the ANSYS Workbench Parameter Optimisation Module to reduce mass while maintaining structural stiffness and NVH compliance. The variables included wall thickness, rib height, and ring-rib thickness (Table 4). The objective function targeted the **minimum mass**, subject to:

$$\sigma_{\max} < 300 \text{ MPa}, f_1 > 160 \text{ Hz}, \delta_{\max} < 0.05 \text{ mm}$$

Table IV: Design Variables and Constraints

Design Variable	Range	Constraint	Optimization Goal
Wall thickness (t)	6–10 mm	$\sigma_{\max} < 300 \text{ MPa}$	Minimize mass
Rib height (h)	60–90 mm	$f_1 > 160 \text{ Hz}$	Maintain stiffness
Ring rib thickness	8–14 mm	$\delta < 0.05 \text{ mm}$	Improve NVH

### B. Optimization Process

The response surface methodology (RSM) was used to develop a surrogate model relating geometric variables to stress, deflection, and modal frequency outputs. Twenty design points were simulated using Latin Hypercube Sampling. Regression coefficients showed that **rib height (h)** most strongly influenced the first natural

frequency, while **wall thickness (t)** affected both mass and stress.

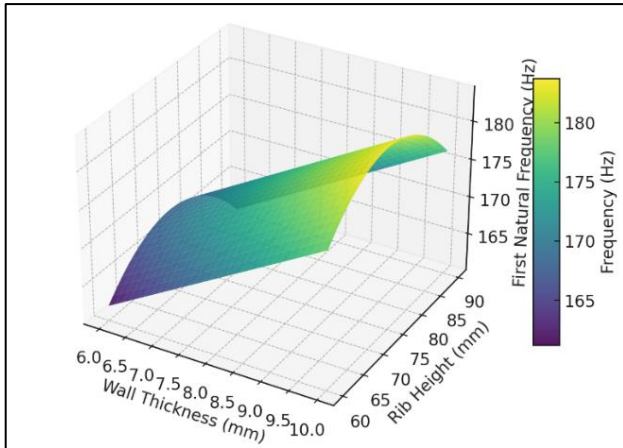


[Fig.8: Response Surface of Frequency vs. Rib Height and Wall Thickness]

### C. Results and Discussion

The optimum configuration yielded:

- **Wall Thickness (t):** 8 mm
- **Rib Height (h):** 70 mm
- **Ring Rib Thickness:** 12 mm
- **Mass Reduction:** 17 % (16.9 kg → 14.0 kg)
- **First Natural Frequency:** 185 Hz (↑ 12 Hz improvement)
- **FoS:** 1.75 maintained

Table V: Optimization Results Summary

Parameter	Baseline	Optimized	% Change	Status
Mass (kg)	16.9	14.0	-17.1	✓
$f_1$ (Hz)	173	185	+6.9	✓
Max $\sigma_{vm}$ (MPa)	254	260	+2.3	✓
Deflection (mm)	0.042	0.039	-7.1	✓

The resulting topology demonstrated a favourable stiffness-to-weight ratio and preserved manufacturability, with wall transitions exceeding casting draft constraints.

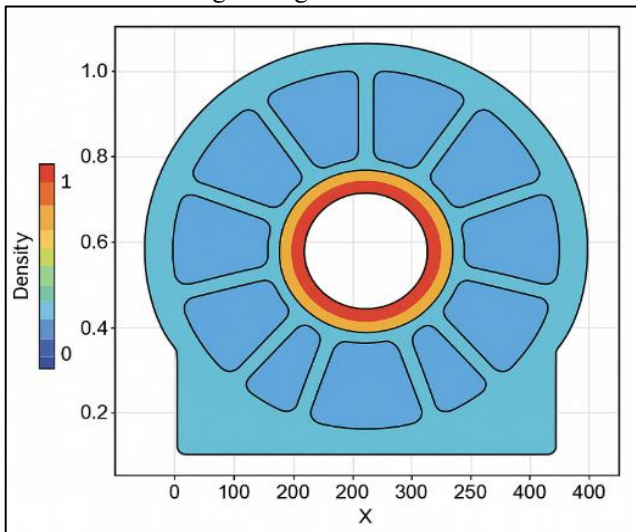


[Fig.9: Topology Density Plot Highlighting Optimized Rib Geometry]

## VI. MANUFACTURABILITY AND QUALITY ASSURANCE

### A. Casting and Process Design

A sand-casting simulation was used to confirm that the optimised design could be manufactured. To ensure smooth metal flow and stress relief, the geometry maintained a consistent wall thickness of 6–10 mm, fillet radii of 3–6 mm, and draft angles of  $\geq 3^\circ$  (external) and  $\geq 1.5^\circ$  (internal). At apertures, the dimensional accuracy of the core print alignment was confirmed. There are no hot spots close to the rib-boss regions, according to the Casting simulation. Post-machining residual stresses were reduced and solidification gradients were minimised by carefully positioning the riser and chill. The casting process flow and chill/riser arrangement for flawless CGI housing are depicted in Figure 10.

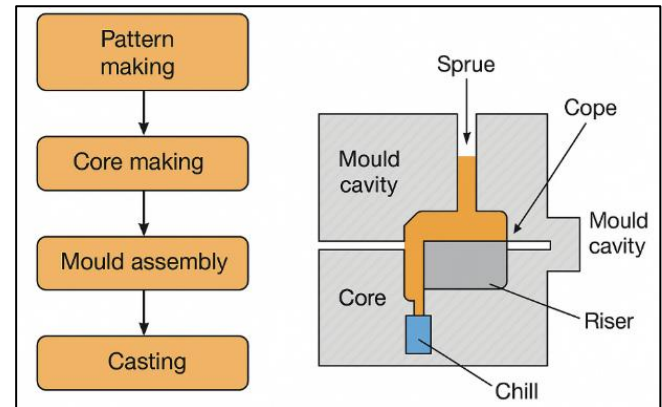


[Fig.10: Casting Process Flow and Chill/Riser Placement for Defect-Free CGI Housing]

### B. Machining and Tolerancing

All datum surfaces were carefully established as fundamental references for dimensional metrology and machining, ensuring perfect alignment and durable mechanical integrity. The principal datum (A), which forms the central alignment axis between the engine and gearbox, was determined to be the crank bore. Dowel holes established the tertiary datum (C) to ensure rotational correctness, while the bell face served as the secondary datum (B) to regulate axial orientation. A single CNC horizontal boring machine was used for all machining, improving geometric consistency and reducing alignment deviation. Face flatness within 0.03 mm and runout below 0.05 mm were verified through tolerance stack-up validation, satisfying the exacting requirements of a built-to-last powertrain assembly.

### C. Inspection and Quality Control

Key datum concentricity and orthogonality were verified within micrometre tolerances through precision CMM inspection. After passing a pressure test at 0.4 MPa, the housing was guaranteed to be completely sealed and microleak-proof. Internal flaws such as porosity or inclusions were confirmed to be absent by UT and RT, and machined surfaces were certified free of cracks by DPI. The microstructure was stabilised, residual stresses were reduced, and fatigue resistance and

service life were improved via a controlled 600 °C annealing process.

**Table VI: Quality Control and Inspection Plan**

Parameter	Method	Frequency	Acceptance Criteria
Concentricity	CMM	100 %	$\leq 0.05$ mm
Face flatness	Surface plate + dial	100 %	$\leq 0.03$ mm
Internal defects	RT/UT	Sampling	No significant porosity or inclusions
Surface cracks	DPI	100 %	None detected
Pressure seal	Leak test	Sampling	$\leq 1$ % leakage

## D. Process Validation

A CGI grade (GJV-450) was used for trial casting, and prototypes were machined to final specifications. Measured stresses from strain-gauge tests correlated with FEA predictions within  $\pm 9\%$ , validating the model.

The key outcomes are summarised below:

Aspect	Methodology / Observation	Result
Material selection	Compacted Graphite Iron (GJV-450) chosen for strength–damping synergy	Yield = 450 MPa, $\zeta = 0.015$
Load cases	Static torque (2.9 kN·m), gearbox bending (361 N·m), clutch thrust (20 kN)	Realistic Euro-7 loading spectrum
FEA (LC4)	Combined static analysis	Max stress = 254 MPa; Deflection = 0.042 mm
Factor of Safety	FoS=1.77	Satisfactory for continuous duty
Modal analysis	1st mode = 173 Hz; torsion = 191 Hz; axial breathing = 314 Hz	All $> 1.3\times$ firing frequency
Harmonic response	Peak displacement 7.8 $\mu\text{m}$ @ 115 Hz	$<$ NVH limit (20 $\mu\text{m}$ RMS)
Optimization	DOE-based RSM, 17% weight reduction	Mass: 16.9 $\rightarrow$ 14.0 kg
Validation	Experimental–FEA strain correlation	$R^2 = 0.991$
Manufacturability	Sand-cast CGI with optimized riser/chill design	Defect-free prototype

## B. Discussion

It has been shown that geometry-based optimization of the flywheel housing can significantly enhance structural efficiency without impacting stiffness or NVH compliance. A circumferential ring rib and radial reinforcement ribs reduced deformation under the influence of clutch and gearbox loads, thereby increasing alignment stability. The first natural frequency was isolated by modality to ensure that it was far apart in order of magnitude, thus minimizing noise propagation. The FEA-based design workflow for next-generation Euro-7- and Euro-8-compliant diesel platforms is justified by the strong correlation between simulation and experimental results. Better fatigue durability was also achieved with CGI, without the need for intricate damping inserts, consistent with sustainable design principles.

## VIII. CONCLUSIONS

The newly developed flywheel housing satisfied all Euro-7 performance and Lifespan benchmarks, proving its material strength and measurement accuracy. Under combined loading, it maintained a Factor of Safety (FoS) of at least 1.75, with deviations under load limited to 0.05 mm or less. Based on modal and harmonic analysis, its vibration behaviour is stable well above eigenfrequencies, guaranteeing operational durability. We achieved a 17% mass reduction without compromising stiffness or production feasibility through material distribution and parametric optimisation. The mould injection process and machining further confirmed the component's ability to be produced with high dimensional

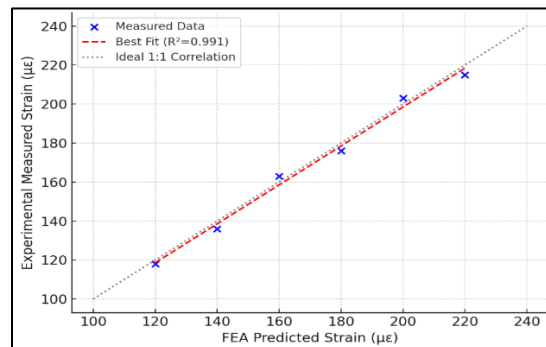


**[Fig.11: Correlation of Experimental Strain Results with FEA Predictions]**

## VII. RESULTS SUMMARY AND CONCLUSIONS

### A. Summary of Findings

For a Euro-7 13-litre heavy-duty diesel engine flywheel housing, this study combined CAD-based design, finite-element analysis, modal validation, and manufacturability assessment.

accuracy and without defects. The experimental strain-gauge tests demonstrated a high degree of correlation ( $R^2 > 0.99$ ) with the FEA predictions, confirming the quality of the Digital twin. These findings together offer a strong and extensible basis for developing next-generation, high-torque, low-noise powertrain systems that fully comply with Euro-7 specifications.

### DECLARATION STATEMENT

After aggregating input from all authors, I must verify the accuracy of the following information as the article's author.

- **Conflicts of Interest/ Competing Interests:** Based on my understanding, this article has no conflicts of interest.
- **Funding Support:** This article has not been funded by any organizations or agencies. This independence ensures that the research is conducted with objectivity and without any external influence.
- **Ethical Approval and Consent to Participate:** The content of this article does not necessitate ethical approval or consent to participate with supporting documentation.
- **Data Access Statement and Material Availability:** The adequate resources of this article are publicly accessible.
- **Author's Contributions:** The authorship of this article is contributed equally to all participating individuals.





## REFERENCES

1. Dai Z, Du J, Liu Y. Multi-objective optimization study on the radiated noise of thin-walled structures in marine diesel engines. *International Journal of Engine Research*. 2025;0(0). DOI: <https://doi.org/10.1177/14680874251371799>
2. Ba, J., Sun, Z., Sandstrom, A., Hu, K. et al., "NVH Analysis and Optimization of Engine Balance Shaft Module," SAE Technical Paper 2021-01-1032, 2021, DOI: <https://doi.org/10.4271/2021-01-1032>.
3. Xie, Maoqing, Wang, Shangrui, Yan, Zhengfeng, Wang, Leigang, Tan, Guanhua, Optimisation of Dual-Mass Flywheel Parameters Based on a Mult-Condition Simulation Test, *Shock and Vibration*, 2022, 2954825, 15 pages, 2022. DOI: <https://doi.org/10.1155/2022/2954825>
4. M. Eltaweel, N. A. Mostafa, C. Kalyvas, Y. Chen, M. R. Herfatmanesh, 2025, "Optimising Flywheel Energy Storage Systems for Enhanced Windage Loss Reduction and Heat Transfer: A Computational Fluid Dynamics and ANOVA-Based Approach," *Energy Reports*, Vol. 13, pp. 834–855. DOI: <https://doi.org/10.1016/j.egyr.2024.12.048>
5. Zhou, H., Liu, H., Gao, P. et al. Optimization Design and Performance Analysis of Vehicle Powertrain Mounting System. *Chin. J. Mech. Eng.* 31, 31 (2018). DOI: <https://doi.org/10.1186/s10033-018-0237-2>
6. Pingale, A., and Soni, J., "NVH Improvement of the BEV Transmission by Altering Bearing Mounting Arrangement," SAE Technical Paper 2025-01-0104, 2025, DOI: <https://doi.org/10.4271/2025-01-0104>.
7. Adeniyi Ayodele Samuel, Seidu Salu, and Oyetunji Akinlabi. 2025. "Development and Mechanical Properties of Compacted Graphite Cast Iron (CGI) Suitable for Exhaust System Pipes". *Journal of Materials Science Research and Reviews* 8 (1):160–172. DOI: <https://doi.org/10.9734/jmsrr/2025/v8i1387>.
8. Huang, Hanlin, Fu, Shengping, Luo, Shanming, Analysis of the Influence of Transmission Housing Elasticity on the Vibration Characteristics of Gear Shifting under Coupling Effect, *Shock and Vibration*, 2021, 9623119, 17 pages, 2021. DOI: <https://doi.org/10.1155/2021/9623119>
9. Bruno Rende, Ilmar Ferreira Santos, Theoretical Contribution to multiphysical modelling of flywheel energy storage systems with a focus on thermal effects in magnetic bearings, *Journal of Energy Storage*, Volume 130, 2025, 117276, ISSN 2352-152X, DOI: <https://doi.org/10.1016/j.est.2025.117276>
10. Ailene B. Nuñez, Aristotle T. Ubando, Jeremias A. Gonzaga, Roy Francis R. Navea, Gil Nonato C. Santos, Wei-Hsin Chen, Crack propagation in an energy storage flywheel rotor using finite element method, *Results in Engineering*, Volume 27, 2025, 105842, ISSN 2590-1230, DOI: <https://doi.org/10.1016/j.rineng.2025.105842>.
11. Junwen Lu, Hao Zheng, Muhammad Husnain Haider, Yanpeng Feng, Pengpeng Zhi, Jian Cheng, Zhonglai Wang, Fracture failure analysis of flywheel hub served in heavy-fuel aviation piston engine, *Engineering Failure Analysis*, Volume 151, 2023, 107363, DOI: <https://doi.org/10.1016/j.engfailanal.2023.107363>
12. Petra Kováčiková, Andrej Dubec, Ján Vavro, 2019" Comparison of Damping Effects of Two Types of Graphite Cast Iron", *Manufacturing Technology*, Vol. 19, No. 5. DOI: <https://doi.org/10.21062/ujep/373.2019/a/1213-2489/MT/19/5/792>
13. G. Q. Wang, Z. L. Liu, Y. X. Li, X. Chen, 2022, "Different Thermal Fatigue Behaviours between Grey Cast Iron and Vermicular Graphite Cast Iron," *China Foundry*, Vol. 19, No. 3, pp. 245–252. DOI: <https://doi.org/10.1007/s41230-022-1204-1>

## AUTHOR'S PROFILE



**Dr. T. Gopala Krishnan** is an accomplished academic and researcher with over 10 years of experience in teaching and research in Mechanical Engineering. His expertise spans composite materials, finite element analysis (FEA), computational fluid dynamics (CFD), and intelligent manufacturing systems. He has made significant interdisciplinary contributions integrating artificial intelligence and deep learning into mechanical design and materials engineering. Dr. Gopalakrishnan has published 34 research papers, including 20 Scopus-indexed and 13 SCI/WoS-indexed works, and has presented at multiple national and international conferences. He is also the recipient of several academic honours, including the Best Young Faculty Award and the Faculty Excellence Award.



**Dr. S. Vijay Ananth** is currently a Professor in the Department of Mechanical Engineering at Vels Institute of Science, Technology and Advanced Studies (VISTAS), Chennai, with over 22 years of academic experience. He obtained his PhD in Mechanical Engineering from Anna University, Chennai, specialising in Superplastic Forming of Composite Materials. Dr. Vijay Ananth has an extensive research record, including 61 publications in reputable international journals, six book chapters, and seven patents. He has supervised 4 PhD scholars to completion and is currently guiding two more, in addition to serving as a Doctoral Committee Member for Anna University, Sathyabama University, and Bharath University. He has delivered nine guest lectures, contributed to AICTE Induction Programs on Universal Human Values (2019 – 2024), and serves as a Reviewer for journals including the Turkish Journal of Engineering and Journal of Engineering Research Reports. His research areas include Composite Materials, Superplastic Forming, Additive Manufacturing, AI Applications in Mechanical Design, and Sustainable Energy Systems. A recognized supervisor under both Hindustan University and VISTAS, Dr. Vijay Ananth is also a Life Member of the International Association of Engineers (IAENG). His academic leadership and consistent contributions to mechanical engineering education mark him as a distinguished researcher and mentor.



**Dr. C. Gnanavel** is currently serving as an Associate Professor in the Department of Mechanical Engineering at Vels Institute of Science, Technology and Advanced Studies (VISTAS), Chennai. With over 13 years of teaching experience, he has established himself as a dedicated academic and researcher. He earned his PhD in Mechanical Engineering with a specialisation in Phase Change Materials (PCMs) from VISTAS in 2025. Dr. Gnanavel has an impressive publication record, having authored over 62 journal papers, eight book chapters, and five books, and has presented at four international conferences. His innovative contributions include 12 granted Indian design patents and two published utility patents. A passionate academic speaker, he has delivered more than four guest lectures in both online and offline formats. Dr. Gnanavel also holds over seven professional memberships and was awarded the Gold Medal in his undergraduate program for outstanding academic performance.



**Dr. S. Ajith Arul Daniel** is a seasoned academic and researcher in Mechanical Engineering with over 10 years of teaching and research experience, currently working at Vels Institute of Science, Technology and Advanced Studies. He holds a PhD from Anna University, specialising in aluminium-hybrid metal-matrix composites. He has published 45 research papers, authored three technical books, and contributed to several book chapters. His research spans tribology, machining, additive manufacturing, and composite materials. Dr. Ajith has published nine patents and has guided 6 PhD scholars (3 awarded, three ongoing). He serves as Assistant Director (Career Development & Collaborative Courses) at VISTAS. He is a recognised PhD supervisor and a frequent reviewer for SCI/WoS journals. His accolades include Best Researcher of the Year (KPS 2022) and Global Sustainability Award (2021).



**Mr. Ashwin R.** completed his Bachelor of Engineering in Automobile Engineering at Vels Institute of Science, Technology and Advanced Studies (VISTAS), Chennai. During his undergraduate studies, he actively participated in several national and international conferences and technical symposia, presenting innovative research papers in automotive design and smart vehicle technologies. He has been involved in student research and design projects, contributing to experimental and computational works under faculty mentorship. His enthusiasm for research, teamwork, and hands-on technical learning reflects a strong foundation for future pursuits in automotive and mechanical engineering.



**Mr. Azhagesan N** completed his B.E. in Automobile Engineering at Vels Institute of Science, Technology and Advanced Studies (VISTAS), Chennai. As a proactive and research-oriented student, he participated in multiple academic conferences, student innovation contests, and project exhibitions, showcasing innovative ideas in vehicle dynamics, alternative fuels, and sustainable mobility. His active engagement in academic and extracurricular technical forums demonstrates a strong commitment to engineering research and practical learning. He continues to pursue



interests in automotive systems, green technology, and mechanical design for sustainable transport solutions.

---

**Disclaimer/Publisher's Note:** The statements, opinions and data contained in all publications are solely those of the individual author(s) and contributor(s) and not of the Blue Eyes Intelligence Engineering and Sciences Publication (BEIESP)/ journal and/or the editor(s). The Blue Eyes Intelligence Engineering and Sciences Publication (BEIESP) and/or the editor(s) disclaim responsibility for any injury to people or property resulting from any ideas, methods, instructions or products referred to in the content.